Hindawi
Mathematical Problems in Engineering
Volume 2022, Article ID 2890035, 12 pages
https://doi.org/10.1155/2022/2890035

Research Article

Study on the Simplification Calculation Model of Marine Diesel Engine Exhaust Flow Based on Air-Fuel Ratio

Guo Junwu and Guo Leyang

Shanghai Maritime University, Marine Merchant College, No. 1550 Haigang Avenue, Shanghai, China

Correspondence should be addressed to Guo Junwu; jwguo@shmtu.edu.cn

Received 28 January 2022; Revised 5 May 2022; Accepted 17 May 2022; Published 13 June 2022

Academic Editor: Adnan Maqsood

Because of the large discharge of marine diesel engines, direct measurement is difficult and complicated. In order to obtain accurate data of marine diesel engine exhaust flow, the carbon balance method is generally used for calculation, but the carbon balance method has iterative operation, adopts wet concentration calculation, and does not consider sulfur oxide components, thus resulting in errors in the calculation results. In this paper, according to the calculation model of air-fuel ratio proposed by S H Chan, the law of conservation of C, H, and O atoms is observed, sulfur oxides in the exhaust are considered, and a new exhaust flow calculation model based on air-fuel ratio is obtained. This calculation model is the first to directly use dry gas concentration in the calculation model of air-fuel ratio. Then, the simplified calculation model is obtained by ignoring CO and simplifying coefficient A^*, the difference between the carbon balance method, ignoring CO, and the simplified model is compared, and then the exhaust flow value and exhaust density are calculated by the test data. The simplified calculation model can also calculate the mass flow rate of carbon dioxide, unburned hydrocarbon, and carbon monoxide. Finally, a software program is developed for the simplified calculation model, which is convenient for quick calculation and quick acquisition of exhaust flow data, thus laying a solid foundation for the application of the simplified calculation model in real ships.

1. Introduction

A lot of domestic and foreign scholars have studied the carbon balance method, and relevant references are listed in the following.

Chen et al. [1] constructed a carbon balance pressure index to measure the eco-environment pressure caused by carbon emissions in 77 countries from 2000 to 2015, and the logarithmic mean Divisia index decomposition method was used to identify the key factors related to carbon balance pressure.

The results of Nichiporovich [2] show that the average daily runoff values are 0.409 mg C/m(2) in the pelagic zone and 0.647 mg C/m(2) in the littoral zone. The balance of carbon dioxide flux shows the universality of runoff over emission.

Chang et al. [3] assume that, under the balanced and optimal economic growth path, the economic growth rate is equal to the consumption growth rate, from which we can obtain the ordinary differential equation governing the consumption level by solving an optimal control problem.

In the paper by Zhang et al. [4], the hybrid graph is proposed to express the direct and indirect constraint relationship among components.

The results of Viglizzo et al. [5] show that grazing lands generate C surpluses that not only could offset rural emissions but also could partially or totally offset the emissions of nonrural sectors.

The results of Uri et al. [6]demonstrate that a well-regenerated young Scots pine stand on a former clear-cut area will be able to turn into a C sequestering ecosystem already before ten years after cutting.

The results of Park et al. [7] show that CH_4 and carbon flow balance methods can be used to estimate model parameters appropriately and to predict long-term carbon emissions from landfills.

The methodology of Crous-Duran et al. [8] is based on comparing the carbon emissions associated with the production of food and the carbon sequestered for that same activity for a particular quantity of food produced over a specific area and over a specific time.

Marin-Muniz and Hernandez [9] outlined a need to conserve and restore wetlands and demonstrated the wetland role as carbon sinks without concerning that they are sources of GHGs.

The results of Daniel et al. [10] indicated that the hydromorphological alterations in these sites might convert healthy ecosystems contributing to C sequestration and climate change mitigation into C-emitting ecosystems.

The work of Morales et al. [11] shows that American Petroleum Institute results have proven to be an efficient tool for practitioners and researchers that intend to analyze the greenhouse gas emission of carbon capture utilization and storage systems to estimate, with accuracy, the global warming impact.

The analysis of Zou et al. [12] shows that the NH_3 emission is highly correlated with the temperature and relative humidity. The ventilation rate shows a positive correlation with all the three gases.

In the paper of Liu et al. [13], their large-scale terrestrial carbon (C) estimating studies using methods such as atmospheric inversion, biogeochemical modeling, and field inventories have produced different results.

The results of Doran-Browne et al. [14] showed that, from 2000 to 2014, Jigsaw Farms reduced its emissions by 48% by sequestering carbon in trees and soil.

The study of Ventura et al. [15] examined the combined effect of woody ash and nitrogen (N) fertilization on the productivity, net C balance (NECB), and soil C sink capacity of a poplar SRC plantation established on a former arable land in northern Italy.

The study by Rasanen et al. [16] explored carbon dioxide fluxes measured with the eddy covariance method for 3 years at a grazed savanna grassland in Welgegund, South Africa.

Weiler et al. [17] used the DayCent model to predict soil C dynamics for the next 30 years under green harvest management in scenarios with 0, 50, and 75% straw removal and to estimate the C savings of different soil tillage methods.

Many domestic and foreign scholars have studied the calculation of diesel engine exhaust flow; relevant references are listed in the following.

In the paper by Liu et al. [18], the calculation formula of the optimal area ratio (K-opt) of outlet and inlet of exhaust port was derived.

Ye et al. [19] numerically simulated the plume field distribution using an ideal jet model and a semiempirical formulation.

Arif et al. [20] proposed a methodology that will allow more accurate analysis of the effects of exhaust nozzle on the overall performance of a unique approach of analyzing jet exhaust nozzle integrated into aircraft and propulsion system.

The experimental and numerical analyses of the standard fume hood features in order to determine the nature of the flow phenomena within the working chamber are presented and studied in the paper of Pietrowicz et al. [21].

In the paper by Pacak et al. [22], a theoretical analysis of heat and mass transfer in a counterflow heat exchanger used for energy recovery in air handling unit (AHU) under subzero operating conditions is presented.

The results by Liu et al. [23] show that the far-field sound pressure level of the tailpipe predicted via the 3D numerical simulation method agrees well with the experimental results, indicating that accurate acoustic parameters of loads can effectively improve the source identification accuracy for an IC engine.

All of the above authors' studies used the carbon balance method to calculate, but the carbon balance method has iterative operation, adopts wet concentration calculation, and does not consider sulfur oxide components, thus resulting in errors in the calculation results. The carbon balance method of diesel engine exhaust flow calculation is very complicated, and the air-fuel ratio model is not used in the calculation of diesel engine exhaust flow. Due to the above shortcomings of the carbon balance method and the existing diesel engine exhaust flow calculation, in order to accurately and quickly calculate the marine diesel engine exhaust flow, this paper conducts further research on the air-fuel ratio calculation model and finally obtains a set of simplified calculation model.

In this paper, based on the calculation model of air-fuel ratio proposed by S H Chan, a new calculation model of air-fuel ratio is obtained by considering the sulfur oxide composition in exhaust gas and a simplified calculation model of exhaust mass flow rate is established.

2. Modified Calculation Model of the Exhaust Flow Based on Air-Fuel Ratio

We know that the exhaust volume of a marine diesel engine is related to the volume change of the cylinder intake and the volume change before and after fuel spray. In the ideal gas condition, the volume change coefficient between the intake and exhaust volume is the coefficient of molecular weight change of the work medium before and after combustion. According to the coefficient of molecular weight change of the work medium before and after combustion, a modified calculation model for the exhaust flow is established.

The specific research ideas are as follows.

According to the characteristics and exhaust components of diesel engines, this paper gets the total exhaust flow with the ratio of air to fuel and then gets the flow of each component according to the proportion of each component.

2.1. The Coefficient of Change of the Molecular Weight of the Working Medium before and after Combustion. From the chemical equation of the reaction, the following are the products obtained from the combustion of a unit mass of fuel:

$$\begin{aligned} N_2&: M_{N_2} = 0.79\psi_a L_0, \\ C&: M_C = \frac{\phi g_c}{12}, \\ CO&: M_{CO} = \frac{\varphi g_c}{12}, \\ CO_2&: M_{CO_2} = (1-\phi-\varphi)\frac{g_C}{12}, \\ H_2O&: M_{H_2O} = \frac{g_H}{2}, \\ O_2&: M_{O_2} = 0.21(\psi_a - 1)L_0 + \frac{1}{2}\varphi\frac{g_c}{12} + \phi\frac{g_c}{12}, \\ L_0 &= \frac{1}{0.21}\left(\frac{m_C}{12} + \frac{m_H}{4} - \frac{m_O}{32}\right), \end{aligned} \tag{1}$$

where g_c is the amount of carbon contained in a unit mass of fuel; g_H is the amount of hydrogen contained in a unit mass of fuel; ϕ is the percentage of carbon expelled as free carbon; φ is the mass fraction of CO in the product; ψ_a is the excess air coefficient; and L_0 is the theoretical air-fuel ratio, which is the amount of air required for complete combustion of a unit mass of fuel calculated according to the chemical equation. It is the minimum amount of air required for the complete combustion of 1 kg of fuel. According to the reaction equation of C, H, and O, considering that 1 kg of fuel already contains oxygen (32 kg/mol), as well as the approximate volume percentages of oxygen and nitrogen in the air of 0.21 and 0.79, respectively, the amount of combustion products is obtained as follows:

$$\begin{aligned} M &= M_{CO_2} + M_{CO} + M_C + M_{N_2} + M_{H_2O} + M_{O_2} \\ &= \frac{g_c}{12} + \frac{g_H}{2} + \frac{\phi g_c}{24} + \psi_a L_0 - 0.21L_0 + \frac{\phi g_c}{12}. \end{aligned} \tag{2}$$

Substituting the expression of the theoretical air-fuel ratio L_0 into the above equation,

$$M = \frac{g_H}{4} + \frac{g_c}{24}(\phi + 2\varphi) + \psi_a L_0 + \frac{m_o}{32}. \tag{3}$$

The volume of the fuel droplets injected into the cylinder is small compared to the volume of the inlet air and is omitted. The work medium before combustion meets $L = \psi_a L_0$. In the exhaust composition of low-speed two-stroke marine diesel engine, the CO concentration accounts for 2.56% of the harmful gas emissions, and the HC concentration accounts for 7.70%.

Therefore, the coefficient of molecular weight change of the work medium is δ.

$$\begin{aligned} \delta &= \frac{M}{L} \\ &= 1 + \frac{g_H}{4L} + \frac{g_C}{24L}(\phi + 2\varphi) + \frac{m_o}{32L}. \end{aligned} \tag{4}$$

2.2. Determining the Air-Fuel Ratio L. The main components of marine fuel are carbon and hydrogen (about 95% or so), plus small amounts of oxygen, nitrogen, sulfur, and metal compounds. Therefore, the molecular formula of fuel oil is represented by "$C_\alpha H_\beta O_\gamma N_\xi S_\zeta$." It is assumed that the main components of air are 78.09% of nitrogen, 20.94% of oxygen, 0.93% of argon, and 0.04% of carbon dioxide. [24].

The equation for combustion (considering air humidity and incomplete combustion and the resulting B) is as follows:

$$\begin{aligned} &C_\alpha H_\beta O_\gamma N_\xi S_\zeta + A(0.7809N_2 + 0.2094O_2 + 0.0093Ar + 0.0004CO_2) \\ &\quad + BH_2O \longrightarrow (v_1CO + v_2CO_2 + v_3O_2 + v_4H_2O + v_5C_ZH_X + v_6H_2 + v_7N_2 + v_8NO + v_9NO_2 + v_{10}Ar + v_{11}SO_2). \end{aligned} \tag{5}$$

or

$$\begin{aligned} &\mathrm{C}_\alpha\mathrm{H}_\beta\mathrm{O}_\gamma\mathrm{N}_\xi\mathrm{S}_\zeta + A^*(3.7292N_2 + O_2 + 0.0444Ar + 0.0019CO_2) + BH_2O \\ &\longrightarrow \begin{pmatrix} v_1CO + v_2CO_2 + v_3O_2 + v_4H_2O + v_5C_ZH_X + v_6H_2 + v_7N_2 + v_8NO \\ +v_9NO_2 + v_{10}Ar + v_{11}SO_2 \end{pmatrix}. \end{aligned} \tag{6}$$

From Dalton's law of partial pressures, it is known that, in an ideal gas mixture, the ratio of the moles of the components is equal to the ratio of the partial pressures [25].

The relationship between air humidity and A^* is given by the following equation:

$$\frac{B}{4.7755A^*} = \frac{p_v}{p - p_v}. \tag{7}$$

p is the total pressure of wet air and p_v is the water vapor partial pressure in wet air. A^*, B, and A are coefficients.

Φ is the ratio of p_v to p_s at the same temperature under the same total pressure state. p_s is the water vapor partial pressure in saturated wet air. Φ is the relative humidity. The following equation is obtained:

$$p_v = \Phi p_s. \tag{8}$$

Equations (7) and (8) can be organized as

$$B = 4.7755 \frac{\Phi p_s}{p - \Phi p_s} A^*. \tag{9}$$

Air-fuel ratio L is expressed as follows:

$$L = \frac{138.325 A^*}{12.011\alpha + 1.008\beta + 15.999\gamma + 14.007\xi + 32.065\zeta}. \tag{10}$$

In formula (10), α is the molecular number of C, β is the molecular number of H, γ is the molecular number of O, ξ is the molecular number of N, and ζ is the molecular number of S.

To find the air-fuel ratio L, we need to first find A^*. The reaction equation of fuel combustion, according to the balance of C, H, O, and N atoms, can be obtained from the following relationship:

$$\alpha + 0.0019A^* = v_1 + v_2 + zv_5, \tag{11}$$

$$2B + \beta = 2v_4 + xv_5 + 2v_6, \tag{12}$$

$$\begin{aligned}(2 + 0.0038)A^* + \gamma + B = {} & v_1 + v_4 + v_8 \\ & + 2\left(v_2 + v_3 + v_9 + v_{11}\right),\end{aligned} \tag{13}$$

$$\xi + 7.4584A^* = 2v_7 + v_8 + v_9. \tag{14}$$

Normally, a particular instrument is not used to measure water vapor concentration alone. If the water vapor condenses on the instrument, it will cause the instrument to not work properly. The usual method used is to remove the water by condensing the sample gas before it reaches the instrument. The resulting gas concentration is thus the dry gas concentration without water vapor [26]. For a given gas, the dry and wet concentration is related as follows:

$$\begin{aligned} y_i^0 &= \frac{y_i}{1 - y_4}, \\ y_i &= \frac{v_i}{\sum_{i=1}^{11} v_i}. \end{aligned} \tag{15}$$

The dry gas concentration is thus expressed as follows:

$$y_i^0 = \frac{y_i}{(1 - y_4)\sum_{i-1}^{11} v_i}. \tag{16}$$

$$v_i = (1 - y_4) y_i^0 \sum_{i=1}^{11} v_i. \tag{17}$$

Therefore, equations (11) to (14) can be expressed as follows:

$$\alpha + 0.0019A^* = \left(y_1^0 + y_2^0 + zy_5^0\right)(1 - y_4)\sum_{i=1}^{11} v_i, \tag{18}$$

$$2B + \beta = \left[2y_4 + \left(xy_5^0 + 2y_6^0\right)(1 - y_4)\right]\sum_{i=1}^{11} v_i, \tag{19}$$

$$\begin{aligned}&(2 + 0.0038)A^* + \gamma + B \\ &\quad = \left[2\left(0.5y_1^0 + y_2^0 + y_3^0 + y_9^0 + y_{11}^0\right)(1 - y_4) + y_4\right]\sum_{i=1}^{11} v_i,\end{aligned} \tag{20}$$

$$\xi + 7.4584A^* = \left(2y_7^0 + y_8^0 + y_9^0\right)(1 - y_4)\sum_{i=1}^{11} v_i, \tag{21}$$

where y_i^0 is the instrumental measurement and A^*, B, y_4, y_6, and $\sum_{i=1}^{11} v_i$ are unknown. To facilitate the solution, new conditions need to be introduced. The reaction equation for the conversion from water gas is expressed as follows:

$$\mathrm{CO} + \mathrm{H_2O} \Longleftrightarrow \mathrm{CO_2} + \mathrm{H_2}. \tag{22}$$

CO and CO_2 concentrations can be related by the equilibrium constant K.

$$K = \frac{(\mathrm{CO_2})(\mathrm{H_2})}{(\mathrm{CO})(\mathrm{H_2O})} = \frac{v_2 \bullet v_6}{v_1 \bullet v_4} = \frac{y_2^0(1 - y_4)y_6^0}{y_1^0 y_4}. \tag{23}$$

K is a function of the equilibrium temperature T_{eq} and has values between 3.5 and 3.8 [27]. Usually, the equilibrium temperature is between 400 K and 3200 K, with the following expression:

$$K = \exp\left[2.743 - \frac{1.761}{0.001T_{eq}} - \frac{1.611}{\left(0.001T_{eq}\right)^2} + \frac{0.2083}{\left(0.001T_{eq}\right)^3}\right]. \tag{24}$$

Solving equations (15) and (25) to (18) and (20) together yields

$$A^* = \frac{\alpha A_1 - \gamma - \left(\alpha A_3 A_4 - K\beta\varphi_{CO_2}/2A_2\right)}{2.0038 + A_5 + 0.00095A_3A_4 - K\varphi_{CO_2}A_5/A_2 - 0.0019A_1}. \tag{25}$$

Among them,

$$A_1 = \frac{\varphi_{CO} + 2\varphi_{CO_2} + 2\varphi_{O_2} + 2\varphi_{SO_2} + \varphi_{NO} + 2\varphi_{NO_2}}{\varphi_{CO} + \varphi_{CO_2} + \varphi_{HC}}, \tag{26}$$

$$A_2 = K\phi_{CO_2} + \varphi_{CO}, \tag{27}$$

$$A_3 = \frac{K\varphi_{CO_2}}{\varphi_{CO}\left(\varphi_{HC} + \varphi_{CO_2} + \varphi_{CO}\right)}, \tag{28}$$

$$A_4 = \frac{X}{Z}\varphi_{CO}\varphi_{HC}, \tag{29}$$

$$A_5 = 4.7755\frac{\Phi p_s}{p - \Phi p_s}. \tag{30}$$

The actual air-fuel ratio can be obtained after formula (22) is brought into formula (10), and the calculation formula for the remaining gases can be obtained. The details are expressed as follows:

$$\varphi_{H_2} = \frac{(2A_1A^* + \beta)\varphi_{CO}\left(\varphi_{CO} + \varphi_{CO_2} + \varphi_{HC}\right) - x\varphi_{CO}\varphi_{HC}\left(\alpha + 0.0019A^*\right)}{2\left(K\varphi_{CO_2} + \varphi_{CO}\right)\left(\alpha + 0.0019A^*\right)}, \tag{31}$$

$$\varphi_{H_2O} = \frac{K\varphi_{CO_2}\varphi_{H_2}}{\varphi_{CO} + K\varphi_{CO_2}\varphi_{H_2}}, \tag{32}$$

$$\varphi_{N_2} = \frac{(7.4584A^* + \xi)\left(\varphi_{CO_2} + \varphi_{HC} + \varphi_{CO}\right)\left(1 - \varphi_{H_2O}\right)}{2\left(1 - \varphi_{H_2O}\right)\left(\alpha + 0.0019A^*\right)} - \frac{\varphi_{NO} + \varphi_{NO_2}}{2}, \tag{33}$$

$$\varphi_{Ar} = \frac{0.0444A^*\left(1 - \varphi_{H_2O}\right)\left(\varphi_{CO} + \varphi_{CO_2} + \varphi_{HC}\right)}{\left(1 - \varphi_{H_2O}\right)\left(\alpha + 0.0019A^*\right)}. \tag{34}$$

2.3. A Correction Factor KW from Dry Basis to Wet Basis Concentration. When calculating the mass flow or volume flow of wet exhaust, if the measured concentration is dry concentration ($conc_D$), it should be converted to wet concentration ($conc_W$) according to the following equation:

$$conc_W = k_w \cdot conc_D, \tag{35}$$

where k_w is the dry (wet) concentration correction factor. k_w can be calculated.

For exhaust, the value of k_w can be determined according to the following equation:

$$K_{w,r} = \left(1 - F_{FH} \cdot \frac{G_{FUEL}}{G_{AIRD}}\right) - K_{w2},$$

$$K_{w2} = \frac{1.608 \cdot H_a}{1000 + \left(1.608 \cdot H_a\right)}, \tag{36}$$

$$H_a = \frac{6.220 \cdot R_a \cdot P_a}{P_B - P_a \cdot R_a \cdot 10^{-2}}.$$

The symbol expression is shown in Table 1.

For the exhaust gas, $K_{w,r}$ can also be determined by the following equation:

$$K_{w,r} = \frac{1}{1 + HTCRAT \cdot 0.005 \cdot \left[\%CO_D + \%CO_{2D}\right]} - K_{w2}. \tag{37}$$

For the intake air, the value of $K_{w,a}$ can be determined according to the following equation:

$$K_{w,a} = 1 - K_{w2}, \tag{38}$$

where $K_{w,a}$ is the dry (wet) correction factor of the inhaled air.

2.4. Determination of the Fuel Consumption per Unit n Mile of the Ship's Main Engine. There is a calculated relationship between the fuel consumption of the main engine per hour as g_f (kg/h), the effective power of the main engine as P_e (kW), and the fuel consumption of the unit effective power output of the main engine per unit time as g_{fP} (kg/kWh) as expressed in the following:

$$g_f = g_{fP} \cdot P_e. \tag{39}$$

Assuming the ship speed V_s (kn, n mile/h), the fuel consumption per nautical mile of the main engine range is expressed as follows:

$$G_f = \frac{g_f}{V_s}. \tag{40}$$

2.5. Determining the Formula for Calculating the Exhaust Flow Rate. If the fuel consumption G_f (kg/n mile) per unit mile of the ship's main engine is known, the exhaust composition of the ship's main engine and the concentration of each component can be obtained by gas detection instruments so that the mass flow rate G_M (kg/n mile) and volume flow rate of the exhaust can be calculated. The calculation equations are expressed as follows:

$$\begin{aligned} G_M &= G_f \cdot \delta \cdot L \\ &= G_f\left(\frac{g_H}{4} + \frac{g_C}{24}(\phi + 2\varphi) + \frac{m_O}{32} + L\right). \end{aligned} \tag{41}$$

The expression for the volumetric flow rate of a gas is expressed as follows:

$$G_V = \frac{G_M}{\rho} = \frac{G_f}{\rho}\left(\frac{g_H}{4} + \frac{g_C}{24}(\phi + 2\varphi) + \frac{m_O}{32} + L\right). \tag{42}$$

Table 1: Expression of symbol.

Symbol	Expression
H_a	Absolute humidity, that is, the mass of water contained in each kg of dry inlet gas (g)
R_a	Relative humidity of the incoming gas (%)
P_a	Saturated vapor pressure of the incoming gas (kPa)
P_B	Total pressure of the incoming gas (kPa)
$K_{w,r}$	The correction factor for the dry (wet) concentration of the original exhaust
K_{w2}	The volume share of water vapor in the wet inlet gas

Another expression for the volumetric flow rate is expressed as follows:

$$G_V = 10^4 G_f \cdot \frac{0.2204K_1 + K_2K_3}{0.2204K_4 - K_3K_5}. \quad (43)$$

In the above equation,

$$K_1 = \frac{\gamma_C M_{CO_2}}{W_C} + \frac{\gamma_N M_{N_2}}{W_{N_2}} + \frac{\gamma_S M_{SO_2}}{W_S},$$

$$K_2 = \gamma_H \frac{W_O}{2W_H} + \gamma_C \frac{2W_O}{W_C} + \gamma_S \frac{2W_O}{W_S},$$

$$K_3 = \frac{0.00042M_{CO_2}}{W_{CO_2}} + \frac{0.822M_{N_2}}{W_{N_2}} + \frac{0.009789M_{Ar}}{W_{Ar}},$$

$$K_4 = 10^6 - 10^4\phi_{O_2} - \frac{1}{2}\phi_{NO} - \frac{1}{2}\phi_{NO_2},$$

$$K_5 = 0.95\frac{W_{O_2}}{M_{O_2}}\left(10^4\phi_{O_2} - \frac{1}{2}\phi_{CO} - \frac{5}{4}\phi_{HC} + \frac{1}{2}\phi_{NO} + \phi_{NO_2}\right), \quad (44)$$

where G_f is the mass flow rate of fuel consumption; γ_C, γ_S, γ_H, and γ_N are the mass fractions accounted for by carbon, sulfur, hydrogen, and nitrogen in the fuel, respectively; W denotes the relative atomic mass or relative molecular mass; M represents the molar volume; and ϕ_{CO}, ϕ_{HC}, ϕ_{O_2}, ϕ_{NO_2}, and ϕ_{NO} represent the dry volume concentrations of CO, HC, O_2, NO_2, and NO in the exhaust, respectively.

2.6. Calculation of the Mass Flow Rate of Each Component Gas. Based on the measured fuel flow and the concentration values of NO_X, HC, CO, CO_2, and O_2, the mass flow rates of each component gas are calculated. The mass flow rates of the main gas components in the exhaust are calculated as indicated in the following:

$$G_{HC} = G_M \times \phi_{HC} \times 4.79 \times 10^{-4}, \quad (45)$$

$$G_{CO} = G_M \times \phi_{CO} \times K_w \times 9.66 \times 10^{-4}, \quad (46)$$

$$G_{NO_x} = G_M \times \phi_{NO_x} \times K_{HDIES} \times 1.587 \times 10^{-3}. \quad (47)$$

ϕ_{HC} and ϕ_{NO_x} are the measured wet basis concentrations expressed in ppm concentrations, or if the NO_X concentration is expressed in dry basis, add K_w to (28).

ϕ_{CO} is the measured dry basis concentration expressed in ppm.

K_{HDIES} is the correction factor for NO_X.

It should be noted that, in the calculation of HC, the C/H ratio is taken as 1 : 1.85. In addition, the coefficients in the NO_X equation are obtained by calculating N_2O, which is the final form of NO_X in the atmosphere.

Based on the exhaust mass flow rate obtained from the previous calculation, the mass flow rate of each component gas can be calculated from the following equation, using CO_2 as an example:

$$G_{CO_2} = \mu\phi_{CO_2}G_M, \quad (48)$$

where G_{CO_2} is the exhaust mass flow rate of CO_2 and μ takes the value 0.1519 when the exhaust density ρ is 1.293 kg/m^3. If the exhaust density ρ is not 1.293 kg/m^3, then the following relationship exists:

$$\mu = \frac{\omega}{\rho}. \quad (49)$$

The parameters μ and ω are taken as shown in Table 2.

3. Test Data Calculation

The test was conducted with a Shanghai Dongfeng G128ZCo high-speed diesel engine, which has a bore of 135 mm, a stroke of 150 mm, a rated speed of 1500 rpm, and a rated power of 162 kW. Table 3 shows the specified experimental modes and weighting factors. The marine diesel engine was tested in accordance with the E3 mode. Table 4 shows the fuel composition and its content in the test. Table 5 shows the test measurement data.

3.1. Calculation of the Air-Fuel Ratio L. According to the composition of the fuel, it can be known that α: β: γ: ξ: ζ is equal to 1 : 1.925 : 0.00087 : 0.001 : 0.0007. $X/Z = 1.85$, K is taken as 3.5, $\alpha = 12$ as the base, $\beta = 23.1$, $\gamma = 0.01$, and the relative molecular mass of the fuel is counted as 168.01. Bringing the data into formulas (10) and (25)–(30), respectively, we can find A_1, A_2, A_3, A_4, A_5, A, and the value of L, as shown in Table 6.

3.2. Calculation of the Fuel Consumption G_f per Unit n Mile for Diesel Engines. Assuming a speed V_s (kn) of 10, according to equation (40), G_f can be obtained as shown in Table 7.

Table 2: IMO calculation formula coefficients.

Gas	μ	ν	ω	Outline quantity
NO_X	1.587	2.053	2.053	Volumetric concentration
CO	0.966	1.25	1.25	Volume concentration
HC	0.479	—	0.619	Volume concentration
CO_2	15.19	19.64	19.64	Percentage
O_2	11.05	14.29	14.29	Percentage

Table 3: Experimental models and weighting factors.

Test cycle type	Rotational speed (%)	Power (%)	Weighting factor
E2 experimental cycle for the "constant speed main propeller" application (including diesel electric drive and all adjustable pitch propeller units)	100	100	0.2
	100	75	0.5
	100	50	0.15
	100	25	0.15
E3 experimental cycle for "main and auxiliary engines operating according to propeller law" application	100	100	0.2
	91	75	0.5
	80	50	0.15
	63	25	0.15

Table 4: Fuel composition and its content.

Mass share of carbon (%)	Mass share of hydrogen (%)	Mass share of sulfur (%)
86.02	13.80	0.18

Table 5: Test measurement data.

Work condition	1	2	3	4
Diesel engine operating parameters				
Power (kW)	162	121.5	82.8	35
Rotational speed (rpm)	1500	1360	1200	900
Torque (N·m)	1800	1090	659.6	370.8
Oil consumption rate (g/kWh)	728.3	587.5	419.1	157.6
Oil consumption (kg/h)	118	71.38	34.7	5.5
Atmospheric environmental parameters				
Ambient pressure (kPa)	100.74	100.75	100.77	100.78
Ambient temperature (°C)	12	12	11.9	11.6
Pressure of water vapor p_s/kPa	1.401	1.401	1.392	1.3401
Relative humidity (%)	60.0	59.7	58.7	58.2
Gas analyzer measured exhaust gas composition and its parameters				
NO_X dry volume concentration	4.48×10^{-4}	3.78×10^{-4}	9.8×10^{-4}	6.5×10^{-4}
SO_2 dry volume concentration	0.07×10^{-4}	0.06×10^{-4}	0.06×10^{-4}	0.07×10^{-4}
C_ZH_X	0.9×10^{-4}	0.9×10^{-4}	0.9×10^{-4}	1×10^{-4}
CO_2 (%)	8.36	6.22	5.3	5
CO	2.7×10^{-4}	2.4×10^{-4}	2.8×10^{-4}	2.4×10^{-4}
O_2 (%)	9.26	12.2	13.7	14.3
Flow speed v (m/s)	0.54	0.68	0.77	0.8
Flow rate V (m^3/s)	0.017	0.022	0.024	0.025
Cavity temperature (°C)	19	18.9	18.9	18.2

Table 6: Air-fuel ratio calculation data.

Parameter calculated value	Parameter calculated value			
A_1	4.2	5.9	7.144	7.686
A_2	29.287	21.794	18.578	17.524
A_3	129.07	145.13	124.1	144.87
A_4	0.00045	0.0004	0.000466	0.00044
A_5	0.0402	0.040	0.0392	0.03725
A^*	31	41.3	48.86	52.1
L	25.27	33.6	39.8	42.47

Table 7: Values of fuel consumption under each operating condition.

Parameter	Numerical value			
Fuel consumption (kg/h)	26	19.32	13.1	5.5
Sailing speed V_s (kn)	10	10	10	10
G_f (kg/n mile)	2.6	1.93	1.31	0.55

3.3. Determine the Mass Flow Rate of Exhaust Gas (kg/n Mile). According to (41) and (45), the mass flow rate values of exhaust gas are shown in Table 8.

3.4. Determine the Volume Flow Rate of the Exhaust Gas (m^3/n Mile). The gas flow rate v (m/s) is measured by the gas analyzer, the cross-sectional area of the pipe S (m^3) can be calculated to obtain the gas flow rate V (m^3/s), the ship's speed under stable working condition is V_s (n mile/h), and the volumetric flow rate of the gas can be obtained as expressed as follows:

$$G_V = 3600 \times \frac{v \cdot S}{V_s}. \tag{50}$$

The calculated data can be obtained as shown in Table 9.

It is found that the average value of the measured exhaust density is 1.2875 kg/m^3, which is not equal to the air density of 1.293 kg/m^3, and the deviation was within 1%, which is within the acceptable range.

4. Simplification of a Calculation Method

The modified method of calculation formula discussed above is complex; for the convenience of calculation and application, it is necessary to simplify the calculation formula.

Due to the low value of CO concentration in the diesel engine, if you do not consider the exhaust CO, an analysis of the formula can find that the product of A_3A_4 terms can exactly eliminate the terms with CO concentration as the multiplier; namely,

$$A_3 \cdot A_4 = K \cdot \frac{X}{Z} \cdot \frac{\phi_{CO_2}\phi_{HC}}{\phi_{CO_2} + \phi_{HC}}. \tag{51}$$

Notated as A', the data are recalculated and obtained as shown in Table 10.

It can be found that, compared with the carbon balance method, the effect of CO concentration on the calculated value of exhaust mass flow is reduced by 1.2% to 1.4%. Therefore, CO can be ignored for the calculation. The comparison of the exhaust mass flow rate calculated by ignoring CO is shown in Figure 1.

Moreover, in the process of calculation, it is found that the denominator part of the A^* expression is calculated very close to 2, and the numerator part of the γ term has a small value, so the expression of A^* can be simplified as shown as follows:

$$A^{*\prime} = \frac{2\alpha A_1 \cdot A_2 + K\beta\phi_{CO_2} - \alpha A_3 \cdot A_4}{4A_2}. \tag{52}$$

The calculated air-fuel ratio data are shown in Table 11.

Table 8: Calculated values of exhaust gas mass flow rate.

Parameter numeric value	Parameter numeric value			
G_M (kg/n mile)	65.8	65	52.2	23.4
G_{ex} (kg/h)	658	650	522	233.8
G'_{ex} (kg/h)	684.3	676.0	542.9	243.15

Table 9: Calculated exhaust density.

Parameter numeric value	Parameter numeric value			
G_M (kg/n mile)	65.8	65	52.2	23.4
G_V (m^3/n mile)	51.8	50.8	40.15	18
ρ (kg/m^3)	1.27	1.28	1.3	1.3

Table 10: Air-fuel ratio data.

Parameter numeric value	Parameter numeric value			
A_1	6.11	6.62	6.87	7.56
A_2	21.35	19.9	19.1	17.53
A'	0.0796	0.09	0.161	0.1926
A_5	0.0735	0.0805	0.0804	0.0777
A'^*	42.5	45.686	47.236	51.3
L'	34.6	37.24	38.5	41.8

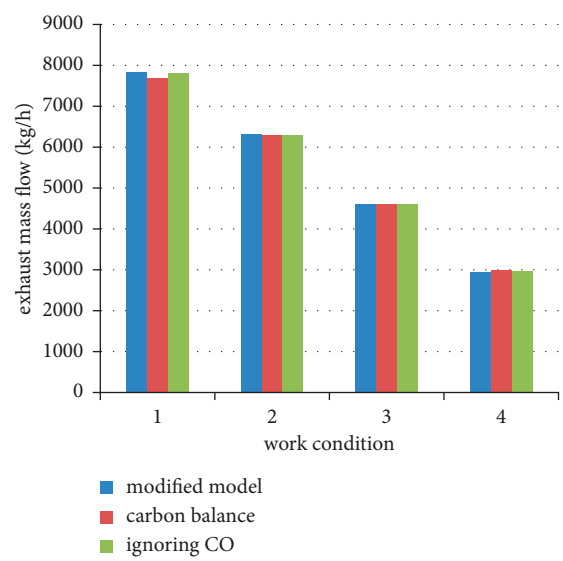

Figure 1: Comparison of the calculated values of the three methods.

A comparison of the exhaust mass flow rate calculated by the simplified model is shown in Figure 2.

It can be found that the calculated values of this simplified model are small compared with the carbon balance method, and the deviations are 2.8%, 4.3%, 4.9%, and 5.6%, respectively. The deviations of the simplified model are all within 10%, which is acceptable due to the requirement of 10% deviation in the NO_X emission specification issued by IMO.

Through experiments under different measurement conditions, it is found that when the simplified calculation model needs more gas components, due to the different measurement accuracy of various instruments, some gas

Table 11: Air-fuel ratio data.

Parameter numeric value	Parameter numeric value			
A_1	6.11	6.62	6.87	7.56
A_2	21.35	19.9	19.1	17.53
A'	0.0796	0.09	0.161	0.1926
$A^{*''}$	42.4	45.5	47	51.1
L''	34.56	37.1	38.3	41.65

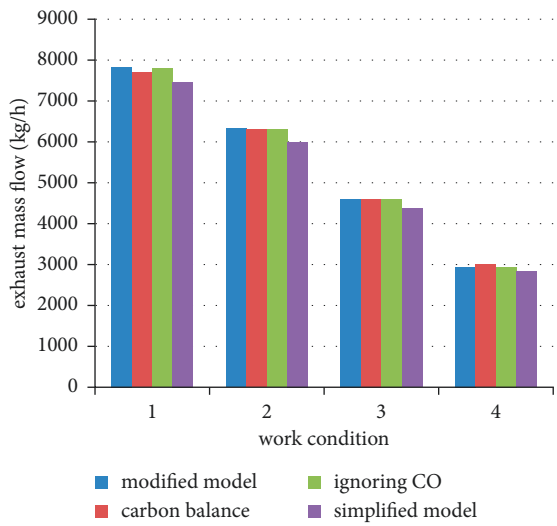

Figure 2: Comparison of the calculated values of the four methods.

Table 12: Software program for this calculation model.

Steps	Command
1	Private sub Command1_Click()
2	X = Val(Text1.Text)
3	Y = Val(Text2.Text)
4	W =vVal(Text3.Text)
5	M = Val(Text4.Text)
6	L = Val(Text5.Text)
7	N = Val(Text6.Text)
8	Z = Val(Text7.Text)
9	$G = 4.9 * (X + L)/(X + Y + \mathrm{N}) + 9.8 * (Y + W + \mathrm{M})/(X + Y + \mathrm{N}) + 5.7 - 5.55 * \mathrm{N} * X/(\mathrm{Y} * Y + Y * \mathrm{N})$
10	$K = Z \quad (0.0366 + G)$
11	Label9.Caption = "" and str(G)
12	Label11.Caption = "" and str(K)

measurement is not accurate, which inevitably leads to a little error in the simplified calculation model. In addition, because the exhaust gas of the diesel engine contains water vapor, the gas concentration measured by the gas analyzer is usually obtained after the removal of water vapor, so there will be some deviation from the real value in the calculation.

5. Development of a Software Program for the Simplification Calculation Method

By analyzing, modifying, and simplifying the calculation model of the exhaust mass flow rate of marine diesel engine and programming it with the computer language Visual Basic, the calculation speed can be greatly improved. The

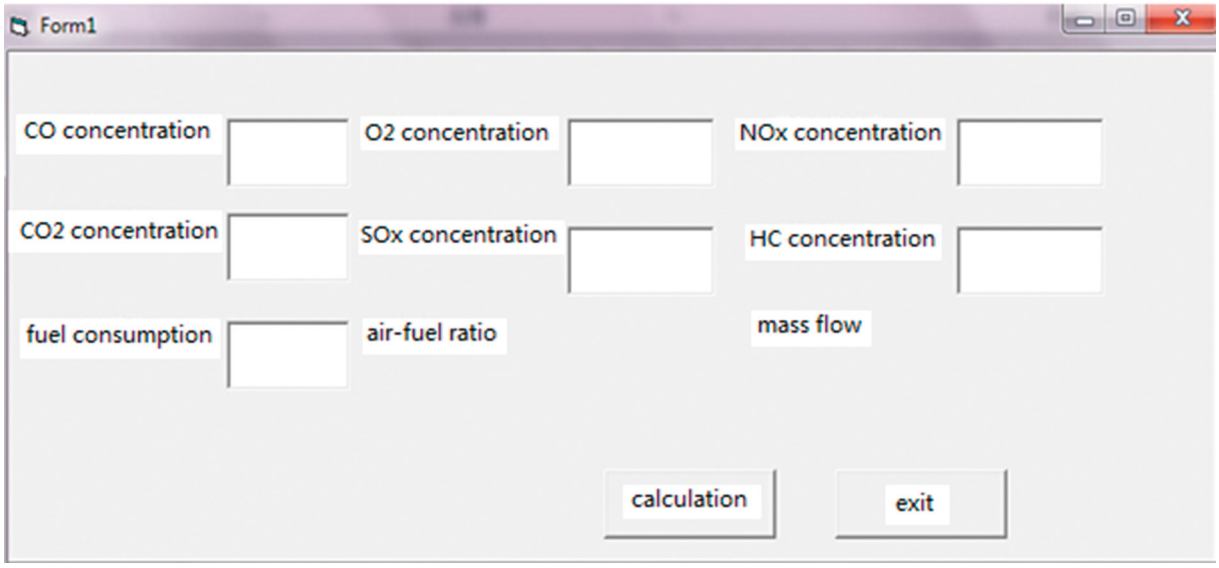

Figure 3: Program interface.

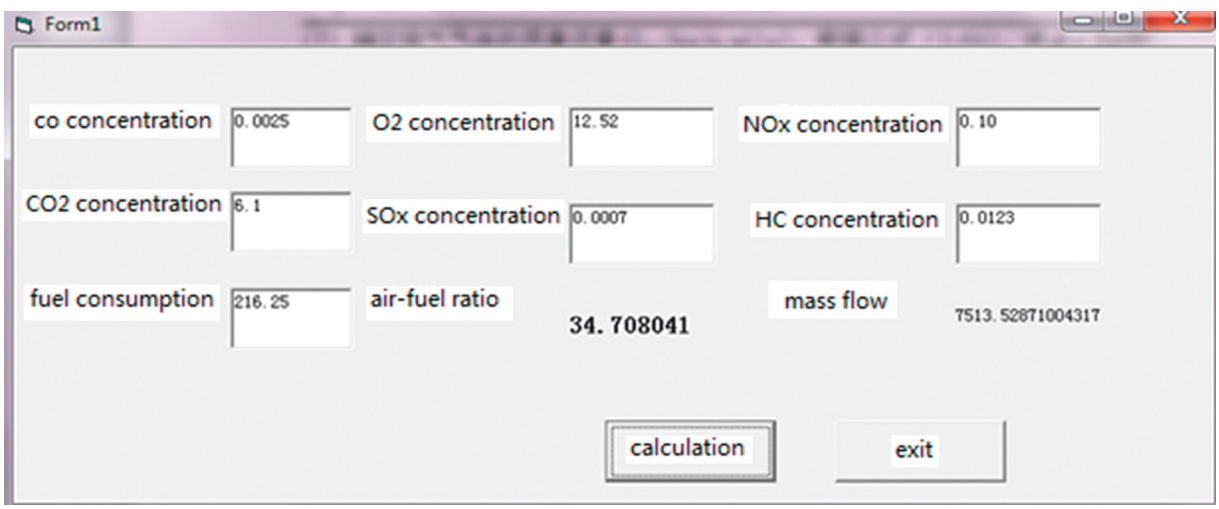

Figure 4: Demonstration of calculation results.

software program for this calculation model is shown in Table 12.

The interface of the designed program and some calculation results are shown in Figures 3 and 4. By running this program, the values of air-fuel ratio and exhaust mass flow rate can be obtained quickly, which is convenient and practical.

6. Conclusions

The model for calculating the exhaust mass flow of marine diesel engines obtained in this paper has the following advantages compared with the carbon balance calculation methods in MARPOL Convention Annex VI.

6.1. Comprehensive Consideration and More Accurate Calculation. The calculation model takes into account the sulfur, nitrogen, and oxygen components in the fuel and is applicable to the calculation of common fuel, while the carbon balance method is only applicable to the fuel containing only hydrogen and carbon components. The correction of the two calculation methods in the MARPOL Convention Annex VI caused by changes in the humidity of the intake air (when the absolute humidity of the intake air is greater than or equal to the humidity of the charge air, i.e., when $Ha \geq Hsc$, part of the water vapor condensates in the intake air) should be made after the exhaust mass flow rate is derived. The modified method corrects the parameters for the wet intake air before the exhaust flow calculation so that the calculated exhaust mass flow is the corrected mass flow. The results are more accurate since the correction is not required to account for the amount of fuel consumed.

6.2. Avoiding the Iterative Operations. The carbon balance method requires iterations of the exhaust density or the wet and dry correction factors for the three cases of each exhaust

component concentration: all wet, all dry, or wet and dry, which may lead to problems of nonconvergence of the iterations. The modified calculation model does not need to consider the iterative calculation when the exhaust concentration is all dry; when the measured concentration is both wet and dry, the problem of iterative nonconvergence will not occur through a one-step correction of the concentration.

Although the simplified calculation method in this paper is based on the carbon balance method, it has its own uniqueness. To avoid iterative calculation, dry concentration is directly used in the calculation formula, which is convenient and fast.

Data Availability

All data, models, and code generated or used during the study are included within the article.

Conflicts of Interest

The authors declare that there are no conflicts of interest regarding the publication of this paper.

Acknowledgments

The authors thank their colleagues for helping them collect the materials and offer many invaluable suggestions. The authors hereby extend their grateful thanks to them for their kind help, without which the paper would not have been what it is. This work was supported by the National Natural Science Foundation of China (Grant no. 11272213).

References

[1] J. Chen, Z. Li, M. Song, and Y. Dong, "Decomposing the global carbon balance pressure index: evidence from 77 countries," *Environmental Science and Pollution Research*, vol. 28, no. 6, pp. 7016–7031, 2020.

[2] V. N. Kudeyarov, "Biogenic carbon balance in the territory of the Russian federation for 1992–2017," *Paleontological Journal*, vol. 54, no. 8, 2020.

[3] S. Chang, X. Wang, and Z. Wang, "Modelling and computing the peaks of carbon emission with balanced growth," *Chaos, Solitons & Fractals: The Interdisciplinary Journal of Nonlinear Science, and Nonequilibrium and Complex Phenomena*, vol. 91, 2016.

[4] L. Zhang, X. Zhao, Q. Ke, W. Dong, and Y. Zhong, "Disassembly line balancing optimization method for high efficiency and low carbon emission," *International Journal of Precision Engineering and Manufacturing-Green Technology*, vol. 8, 2019.

[5] E. F. Viglizzo, M. F. Ricard, M. A. Taboada, and G. Vázquez-Amábile, "Reassessing the role of grazing lands in carbon-balance estimations: meta-analysis and review," *The Science of the Total Environment*, vol. 661, 2019.

[6] V. Uri, K. Mai, J. Aosaar et al., "The carbon balance of a six-year-old Scots pine (Pinus sylvestris L.) ecosystem estimated by different methods," *Forest Ecology and Management*, vol. 433, 2019.

[7] J.-K. Park, Y.-G. Chong, K. Tameda, and N.-H. Lee, "Applying methane and carbon flow balances for determination of first-order landfill gas model parameters," *Environmental Engineering Research: Environmental Engineering Research*, vol. 25, no. 3, 2020.

[8] J. Crous Duran, A. R. Graves, S. Garcia de Jalón, J. A. Paulo, M. Tomé, and J. H. N. Palma, "Assessing food sustainable intensification potential of agroforestry using a carbon balance method," *Forest - Biogeosciences and Forestry*, vol. 12, no. 1, 2019.

[9] J. L. Marin-Muniz and M. E. Hernandez, "Carbon balance in tropical freshwater wetlands on the coastal plain of the Gulf of Mexico," *Limnética*, vol. 39, no. 2, 2020.

[10] M. Daniel, P. Antonio, R. Carlos, C. Santamans Anna, L. J. Miralles, and C. Antonio, "Influence of the conservation status on carbon balances of semiarid coastal Mediterranean wetlands," *Inland Waters*, vol. 10, no. 4, 2020.

[11] M. Mam, V. Fcp, D. Sam, and L. Ma, "Comparison of carbon balance measuring tools in an enhanced oil recovery project based on the carbon dioxide from the ammonia production process streams," *Journal of Cleaner Production*, vol. 144, no. 2, pp. 540–552, 2017.

[12] B. Zou, Z. Shi, and S. Du, "Gases emissions estimation and analysis by using carbon dioxide balance method in natural-ventilated dairy cow barns," *International Journal of Agricultural and Biological Engineering*, vol. 13, no. 2, 2020.

[13] J. Liu, B. M. Sleeter, Z. Zhu et al., "Critical land change information enhances the understanding of carbon balance in the United States," *Global Change Biology*, vol. 26, no. 7, pp. 3920–3929, 2020.

[14] N. Doran-Browne, M. Wootton, C. Taylor, and R. Eckard, "Offsets required to reduce the carbon balance of sheep and beef farms through carbon sequestration in trees and soils," *Animal Production Science*, vol. 58, no. 9, 2018.

[15] M. Ventura, P. Panzacchi, E. Muzzi, F. Magnani, and T. Giustino, "Carbon balance and soil carbon input in a poplar short rotation coppice plantation as affected by nitrogen and wood ash application," *New Forests*, vol. 50, no. 6, 2019.

[16] M. Räsänen, M. Aurela, V. Vakkari et al., "Carbon balance of a grazed savanna grassland ecosystem in South Africa," *Biogeosciences*, vol. 14, no. 5, 2017.

[17] A. W. Douglas, J. M. Vagner, O. A. Gabriel et al., "Carbon balance in sugarcane areas under different tillage systems," *BioEnergy Research*, vol. 12, no. 6, 2019.

[18] F. Liu, Y. Xu, J. Rui, Z. Shi, and Y. Li, "Flow analysis and theoretical design of diesel engine exhaust port," *International Journal of Automotive Technology*, vol. 21, no. 1, 2020.

[19] S. Ye, S. Li, W. Xiong et al., "Calculation and simulation on NIR hyperspectrum of engine exhaust plume," *Spectroscopy and Spectral Analysis*, vol. 37, no. 9, 2017.

[20] I. Arif, J. Masud, and S. Shah, "Computational analysis of integrated engine exhaust nozzle on a supersonic fighter aircraft [J]," *Journal of Applied Fluid Mechanics*, vol. 11, no. 6, 2018.

[21] S. . Pietrowicz, P. Kolasiński, and M. Pomorski, "Experimental and numerical flow analysis and design optimization of a fume hood using the CFD method," *Chemical Engineering Research and Design*, vol. 132, 2018.

[22] P. Anna, A. Jedlikowski, M. Karpuk, and S. Anisimov, "Analysis of power demand calculation for freeze prevention methods of counter-flow heat exchangers used in energy recovery from exhaust air," *International Journal of Heat and Mass Transfer*, vol. 133, 2019.

[23] H. Liu, Y. Chen, and X. Qian, "Numerical and experimental analysis of the effect of acoustic loads on the source

characterization for an internal combustion engine exhaust system," *IEEE Access*, vol. 8, 2020.

[24] J. Liu and Q. Su, "Study on determining air-fuel ratio according to emission composition," *Transactions of CSICE*, vol. 3, no. 18, pp. 308–311, 2000.

[25] W. Shen and J. Tong, *Engineering Thermodynamics*, pp. 367–380, Higher Education Press, Beijing, fourth edition, 2007.

[26] S. H. Chan, "An exhaust emissions based air-fuel ratio calculation for internal combustion engines," *Proceedings of the Institution of Mechanical Engineers - Part D: Journal of Automobile Engineering*, vol. 210, no. 3, pp. 273–280, 1996.

[27] Y. Park and E. S. Richard, "Thermodynamic properties of ideal gas air," *International Journal of Energy Research*, no. 9, pp. 5–7, 1996.